Airport Pavement Inspection through Multi-Static GPR Surveys Using Deep Neural Networks

Lilong Zou
Faculty of Engineering, Computing and the Environment
Kingston University
London, UK
l.zou@kingston.ac.uk

Ying Li
School of Computing and Mathematical Sciences
Birkbeck, University of London
London, UK
ying.li1@bbk.ac.uk

Kevin Munisami
Faculty of Engineering, Computing and the Environment
Kingston University
London, UK
j.munisami@kingston.ac.uk

Amir M. Alani
Faculty of Engineering, Computing and the Environment
Kingston University
London, UK
m.alani@kingston.ac.uk

Motoyuki Sato
Tohoku University
Sendai, Japan
motoyuki.sato.b3@tohoku.ac.jp

***Abstract*—A novel method for airport pavement inspection was proposed, combining multi-static Ground Penetrating Radar (GPR) data with deep learning techniques. The study utilized the Markov Transition Field (MTF) to transform GPR time-series data into two-dimensional images suitable for analysis by Convolutional Neural Networks (CNNs). This framework enabled the automatic detection and classification of interlayer debonding in pavements. Experimental validation was conducted using real-world data from Haneda International Airport, demonstrating the capability of the proposed method to accurately identify debonding regions. The results highlighted the framework's efficiency and reliability in monitoring airport pavements, making it a promising tool for infrastructure maintenance and management.**

Keywords—multi-static Ground Penetrating Radar (GPR), airport pavement, Markov Transition Field (MTF), Convolutional Neural Networks (CNNs), pavement debonding

I. INTRODUCTION

The structural integrity and functionality of airport pavements are considered essential for ensuring the safety and efficiency of air transport systems. Significant stresses are experienced by these pavements due to high aircraft loads and frequent traffic, necessitating regular monitoring and maintenance activities. Traditional inspection methods, including visual inspections and core sampling, are regarded as time-consuming and disruptive while often being limited in providing a detailed understanding of subsurface conditions. In recent years, the use of non-destructive testing (NDT) techniques such as Ground Penetrating Radar (GPR) has been increasingly adopted. These techniques are valued for their ability to provide rapid and high-resolution subsurface data without causing damage to the pavement structure [1][2].

GPR surveys are employed to utilize electromagnetic wave propagation for the detection of subsurface anomalies, including voids, cracks, and moisture infiltration within pavement layers. The application of multi-static GPR configurations has been designed to enhance data richness, as multiple antennas are used for both transmission and reception of signals simultaneously. This approach ensures that diverse perspectives on the subsurface features are obtained, which contributes to a more comprehensive understanding of the underground conditions [3]. However, despite these advancements in technology, the interpretation of GPR data continues to pose significant challenges. The complexity and high-dimensional nature of the data require sophisticated processing and analysis techniques to extract meaningful insights effectively. As a result, ongoing efforts are being made to refine methods for data interpretation and improve the reliability and accuracy of GPR surveys in various engineering and construction applications.

The field of GPR data analysis has been significantly transformed by the emergence of deep learning, which has introduced innovative methods for automation and enhancement. The application of Convolutional Neural Networks (CNNs) has been widely recognized for achieving exceptional performance in various domains, including image classification, object detection, and semantic segmentation. These advanced capabilities allow CNNs to excel in identifying and extracting meaningful patterns from complex GPR datasets. It is believed that these methods have the potential to surpass traditional signal-processing techniques in both efficiency and accuracy. Despite these advancements, the use of CNNs in the context of GPR data analysis for the purpose of airport pavement inspection has not been sufficiently explored. Considerable opportunities remain to investigate how these technologies can be applied effectively in this area. The underutilization of CNNs in such a critical application highlights the need for further research to fully leverage their potential for improving inspection processes [4][5].

A novel framework for airport pavement inspection is introduced in this paper, integrating multi-static GPR surveys with deep neural networks. The spatial diversity of multi-static GPR data is utilized alongside the powerful feature extraction capabilities of CNNs. Through this integration, the approach seeks to provide accurate and automated assessments of pavement health. The methodology involves several key steps, including data preprocessing, network training, and validation. Real-world GPR datasets, collected from airport pavements, are employed to validate the framework. The findings indicate that the proposed framework enhances both efficiency and reliability in airport pavement inspections. This approach demonstrates its potential to streamline the inspection process, reduce manual intervention, and deliver consistent evaluations. The results underline the importance of combining advanced imaging techniques with machine learning to address challenges in infrastructure monitoring and maintenance.

II. METHODOLOGY

A. Airport pavement structure

An airport pavement shallow structure is regarded as a simplified system developed to accommodate the movement of aircraft while distributing loads effectively to the layers beneath. This structure is engineered to maintain both durability and functionality over time. Typically, it is composed of several key layers, including a surface layer made of either asphalt or concrete, a semirigid base course formed from granular or stabilized material, and a subbase layer, as shown in Figure 1. These components rest on a carefully compacted earth subgrade. The layers are designed to work in unison to endure the significant stresses imposed by heavy aircraft loads. Additionally, resistance to environmental factors, such as freeze-thaw cycles, is provided, ensuring longevity and reliability. Smooth, skid-resistant surfaces are also delivered by this system, contributing to safe aircraft operations. The shallow pavement structure plays a vital role in maintaining operational safety and efficiency, meeting the rigorous demands placed on modern airport facilities [6].

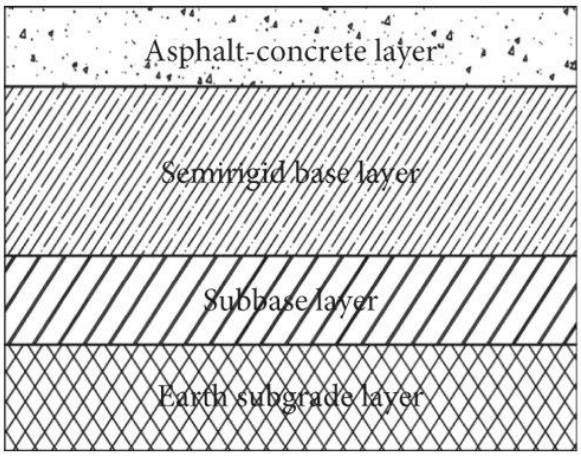

Fig. 1. Typical airport pavement structure.

Debonding in airport pavements is characterized by the weakening or failure of the bond between layers, such as the surface and base, resulting in reduced structural integrity and diminished performance. This issue is frequently encountered due to the improper application or substandard quality of bonding agents, including tack coats. The presence of contaminants, such as dust or moisture, at the interface during construction is known to exacerbate this problem. Furthermore, insufficient compaction during the construction process has been observed to increase the likelihood of debonding. Heavy aircraft loads and temperature fluctuations often lead to shear stresses and repetitive expansion-contraction cycles, which intensify the separation between pavement layers. Aging, material incompatibility, and prolonged environmental exposure also contribute to the progressive deterioration of the bond. Debonding is typically observed at the interface between the asphalt layer and base layer or between the base layer and subbase layer. Preventive measures, such as meticulous surface preparation, careful material selection, and adherence to optimal construction practices, are considered essential to mitigate this issue. These steps are vital to ensuring the durability and long-term performance of airport pavements, thereby reducing maintenance costs and enhancing safety.

B. Numerical modeling and interlayer debonding

To generate the training data set, a three-dimensional forward modeling process based on the finite-difference time-domain method was conducted. The dimensions of the road structure model were configured as 2.0 meters by 2.0 meters by 0.7 meters. This configuration was chosen to balance simulation accuracy and computational efficiency. Debonding commonly occurs at the interface between the asphalt layer and the base layer or between the base layer and the subbase layer. Two types of materials were introduced into the debonding region: water and air.

Debonding may take place in a single area or in two areas simultaneously. Based on these possibilities, nine sets of forward modeling parameters were applied in this study. These include the following scenarios: no debonding, debonding at the interface between the asphalt layer and the base layer with either air or water as the infill material, debonding at the interface between the base layer and the subbase layer with either air or water as the infill material, and debonding at both interfaces with combinations of air-air, air-water, water-air, and water-water as infill materials.

Each forward model underwent 400 simulations. During these simulations, slight variations were introduced to the model parameters, such as the thickness of the structure, the size of the debonding region, the roughness of the interface boundary, and the dielectric constants of the materials. These variations were incorporated to ensure the model could adapt to diverse conditions. The arrangement of the transmitting and receiving antennas was aligned with the configuration of a practical multi-static GPR system.

The antennas were positioned 2 centimeters above the surface of the roadbed, reflecting realistic measurement scenarios more closely. This approach ensured the fidelity of the simulations to actual conditions. Through this modeling process, a comprehensive set of training data was generated to support further analysis and applications. Simulations and parameter adjustments were carefully managed to achieve optimal outcomes.

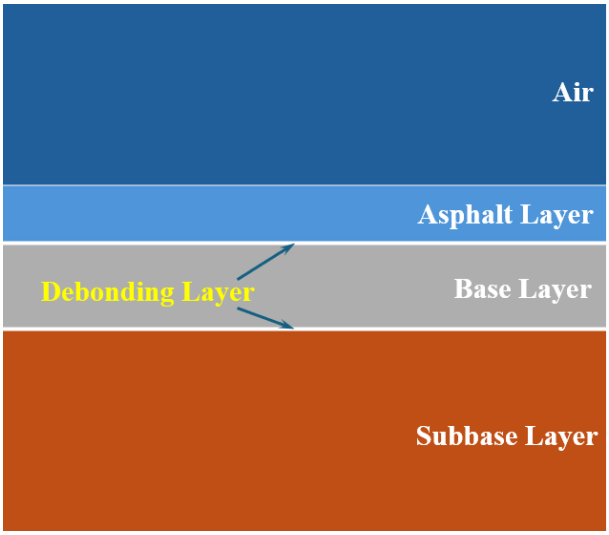

Fig. 2. Schematic of the 3D FDTD model.

C. Markov Transition Field

To maximize the benefits of CNNs in image processing, a method for converting multi-static GPR responses into two-

dimensional (2D) images must be developed. These images can then be effectively analyzed using CNNs. One promising approach involves the use of the MTF, which has been identified as an effective technique. Through this method, one-dimensional (1D) time series data are transformed into 2D images, enabling compatibility with machine learning models. CNNs, recognized for their superior performance in image data processing, particularly benefit from such transformations. The fundamental principle underlying MTF involves capturing temporal dynamics within the time series. This is achieved by encoding the transition probabilities between various states of a Markov process. The outcome of this process is a structured image representation that preserves the temporal features of the original data, ensuring suitability for advanced image analysis techniques [7].

In this study, the MTF algorithm is applied to transform one-dimensional spectral data from GPR into a two-dimensional image format. The process is carried out through several critical steps. Initially, multi-static GPR data from various types of debonding pavement structures is gathered and normalized. The GPR data for each offset is represented as $X = \{x_1, x_2, x_3, \dots, x_m\}$, where n denotes the total number of signal points. Subsequently, reflection signal quantiles are defined. For the given data sequence X, a specific quantile Q is selected, and each signal value q_i is assigned to a corresponding quantile q_j , with j belonging to the range $[1, Q]$.

The construction of a $Q \times Q$ Markov transition matrix is undertaken in the next step. This matrix is developed based on the quantiles derived in the previous step. Transition probabilities between first-order Markov chains are calculated to populate the matrix. As a result, a final representation of the transition dynamics of the GPR data is obtained in a two-dimensional format. This transformed data is designed to be suitable for further analysis, particularly for use in deep learning applications. Through this method, the mapping of GPR spectral data into a two-dimensional space is effectively achieved [8].

$$M = \begin{bmatrix} \omega_{ij}|_{x_1 \in q_i, x_1 \in q_j} & \cdots & \omega_{ij}|_{x_1 \in q_i, x_n \in q_j} \\ \omega_{ij}|_{x_2 \in q_i, x_1 \in q_j} & \cdots & \omega_{ij}|_{x_2 \in q_i, x_n \in q_j} \\ \cdots & \ddots & \cdots \\ \omega_{ij}|_{x_n \in q_i, x_1 \in q_j} & \cdots & \omega_{ij}|_{x_n \in q_i, x_n \in q_j} \end{bmatrix} \quad (1)$$

where, q_i and q_j are the quantiles corresponding to x_i and x_j, respectively. Then, the final output M_{sum} will be generated with following formulation:

$$M_{sum} = \sum_{k=1}^{n} M_k$$

where, k indicates multi-static channel and n indicates the channel number.

D. Convolution Neural Network

CNN is recognized as one of the significant algorithms in the domain of deep learning. Its design allows for the sharing of receptive domains and weights, which reduces the number of neural network parameters requiring training. This reduction simplifies the overall complexity of the model when compared with traditional artificial neural networks. As a result, these networks exhibit unique strengths in tasks such as image processing, target detection, and target tracking. Over recent years, CNN learning algorithms have been applied successfully across numerous fields [9].

A complete convolutional neural network is typically composed of four key components: a convolutional layer, an activation layer, a pooling layer, and a fully connected layer. The convolutional layer consists of several convolution kernels. Within the network, this layer assumes the critical role of extracting features from input images. Initially, basic features, such as edges and shapes, are extracted in the early layers. As the depth of the network increases, subsequent layers focus on identifying increasingly complex and specific features. Following the convolutional layer, the activation layer is generally included to map results in a nonlinear manner.

The pooling layer performs dimensionality reduction of feature vectors, contributing to enhanced efficiency. The fully connected layer, positioned toward the end of the network, is tasked with making final predictions or classifications. These layers work in harmony to optimize the performance of the network. Structures of convolutional neural networks, such as the one depicted in Figure 3, have been specifically designed to facilitate the efficient monitoring of airport pavement debonding.

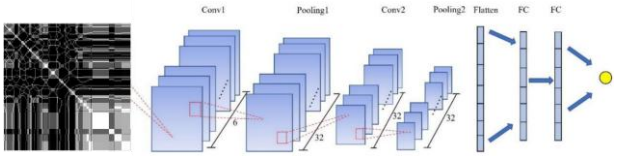

Fig. 3. The designed structure of 2DMTF CNN.

III. Field Experiments and Results

A. Field Experiement

The measurement was carried out on the taxiway asphalt pavement at Haneda International Airport to test the feasibility of the proposed approach. The measurement site is shown in Figure 4. The size of the entire measurement area was around 20 square meters. The data consisted of three parallel multi-

Fig. 4. Measurement map of Haneda International Airport.

static GPR acquisitions along the direction of the aircraft

moving. We chose the survey area that contained the known sound pavement and the interlayer debonding pavement parts. The interlayer debonding occurring areas located at 4 to 6 m in the *x*-direction (survey direction) and 4.5 to 5.5 m in the *y*-direction (the cross-survey direction), was shown as white circles in Figure 4.

B. Training Results of CNN Models

An NVIDIA GeForce RTX3080 GPU, along with the MATLAB deep learning toolbox, was utilized for the training, validation, and testing of the proposed approach for detecting debonding layers. The training process employed all MTF images generated from the nine simulation group models, as shown in Figure 5. None indicates no debonding occurs in this region, Air or water indicate that air or water were filled in the debonding region. In Figure 6, the loss function associated with the proposed model during training is depicted. Similarly, Figure 7 illustrates the accuracy function of the model throughout the training process. A continuous decrease in the loss value was observed as the training iterations progressed, accompanied by a steady increase in the accuracy value. Both metrics exhibited stabilization after 400 iterations. This stabilization highlights the strong training performance of the proposed model. Moreover, a high convergence rate was achieved through the application of pretraining parameters. These results demonstrate the effectiveness of the training methodology and indicate that the model is well-suited for the intended task. The ability of the model to achieve stability and optimal performance in a relatively small number of iterations reflects the robustness of the approach employed. Overall, the training process ensured the reliable development of a model capable of accurately detecting debonding layers in simulation images.

After the training process, the CNN model was saved and tested using a real measurement GPR dataset. The identified types and positions of debonding layers were presented in Table I by the proposed methodology. From the results, it can be observed that a significant portion of the measured pavement was detected as exhibiting debonding phenomena by the trained MTF-CNN model. Within the detected regions, two debonding layers were identified, and the filled material was classified as air-air and water-water. Meanwhile, the majority of the measurement area was recognized as healthy pavement, aligning more closely with the actual condition. This indicates that the trained model successfully distinguished between areas with and without debonding, demonstrating its effectiveness in identifying pavement health. The results highlight the model ability to provide accurate detection, making it suitable for real-world applications in pavement analysis and maintenance planning.

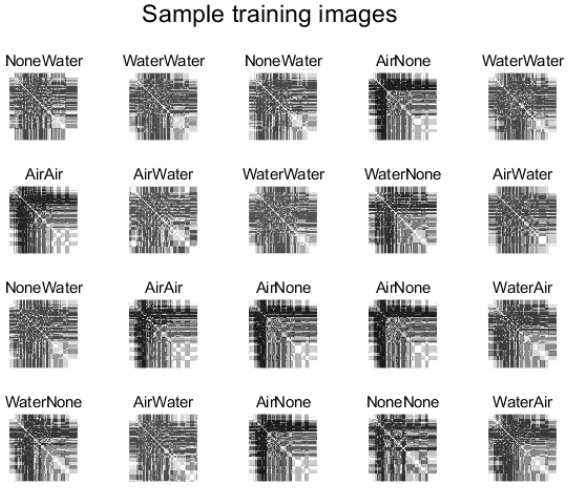

Fig. 7. The training images generate by MTF with simulated data.

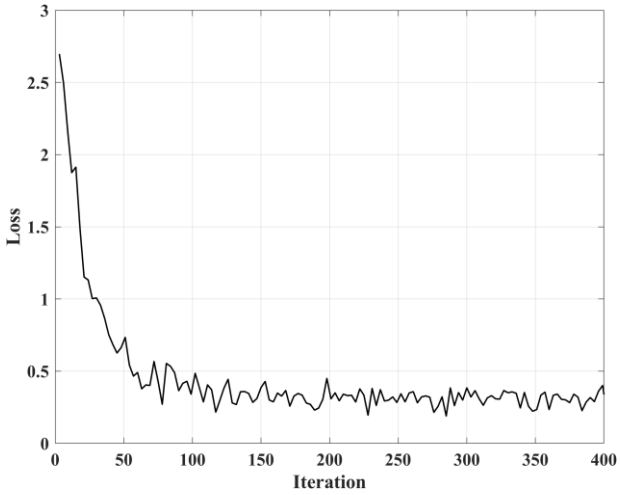

Fig. 5. Loss curve of the proposed trainning CNN model.

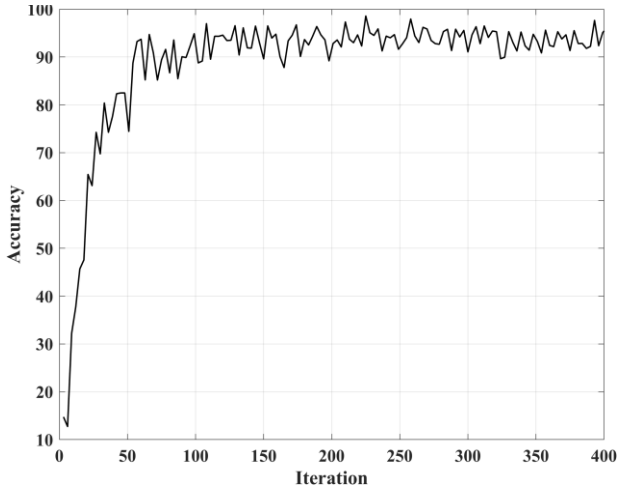

Fig. 6. Accuracy curve of the proposed trainning CNN model.

IV. CONCLUSIONS

In this study, a novel intelligent method for diagnosing airport pavement debonding was proposed, utilizing the Markov transition field (MTF) and a residual network. The process involved the encoding of multi-static GPR time-series signals into two-dimensional images through the use of Markov transition fields. This approach allowed the time dependence of the original signals to be preserved while eliminating the need for prior knowledge to set parameters during the conversion. On this foundation, a convolutional neural network (CNN) was employed to classify images and identify fault types effectively. Experiments conducted on the Hanada International Airport dataset demonstrated that the MTF-CNN method delivered excellent performance in identifying debonding layers with varying severities and locations. When compared to other methods, the MTF-CNN technique provided an automatic capability for feature extraction and classification, enhancing the accuracy and efficiency of the debonding diagnosis process.

TABLE I. DETECTED DEBONDING RESULTS

Number	Position		Type
	X direction	***Y Direction***	
1	5.12 m	4.56 m	Air-Air
2	5.36 m	4.56 m	Air-Air
3	4.08 m	4.92 m	Air-Air
4	4.58 m	4.92 m	Air-Air
5	4.78 m	4.92 m	Air-Air
6	5.24 m	4.92 m	Air-Air
7	2.92 m	5.64 m	Air-Air
8	4.50 m	5.04 m	Air-Air
9	4.62 m	5.04 m	Air-Air
10	4.76 m	5.04 m	Air-Air
11	2.84 m	4.44 m	Water-Water
12	2.88 m	4.44 m	Water-Water
13	2.90 m	4.44 m	Water-Water
14	2.92 m	4.44 m	Water-Water
15	3.06 m	4.56 m	Water-Water
16	2.84 m	4.56 m	Water-Water
17	2.94 m	4.56 m	Water-Water
18	3.14 m	4.56 m	Water-Water
19	3.22 m	4.68 m	Water-Water
20	2.76 m	4.68 m	Water-Water
21	2.88 m	4.68 m	Water-Water
22	1.24 m	5.88 m	None-None
23	5.64 m	6.00 m	None-None
24	3.28 m	3.26 m	None-None
25	2.36 m	3.48 m	None-None

REFERENCES

[1] A. Benedetto and L. Pajewski, Civil Engineering Applications of Ground Penetrating Radar. Springer, 2015.

[2] L. Zou H. Liu, A.M. Alani and G. Fang, "Surface Permittivity Estimation of Southern Utopia Planitia by High-Frequency RoPeR in Tianwen-1 Mars Exploration," IEEE Trans. Geosci. Remote Sens., vol. 62, pp. 1–9, Feburary 2024.

[3] L. Zou, L. Yi and M. Sato, "On the use of lateral wave for the interlayer debonding detecting in an asphalt airport pavement using a multistatic GPR system," IEEE Trans. Geosci. Remote Sens., vol. 58, no. 6, pp. 4215- 4224, January 2020.

[4] H. Liu, Y. Yue, C. Liu, B. F. Spencer, and J. Cui, "Automatic recognition and localization of underground pipelines in GPR B-scans using a deep learning model," Tunn. Undergr. Space Technol., vol. 134, pp. 104861, April 2023.

[5] H. Liu, C. Lin, J. Cui, L. Fan, X. Xie, and B. F. Spencer, "Detection and localization of rebar in concrete by deep learning using ground penetrating radar," Autom. Constr., vol. 118, pp. 103279, October 2020.

[6] K.R. Maser, "Condition assessment of transportation infrastructure using ground-penetrating radar," J. Infrastruct. Syst., vol. 2, pp. 94-101, June 1996.

[7] R. Li, Y. Wu, Q. Wu, N. Dey, R.G. Crespo and F. Shi, "Emotion stimuli-based surface electromyography signal classification employing Markov transition field and deep neural networks," Measurement, vol. 189, pp. 110470, February 2022.

[8] B. Han, H. Zhang, M. Sun and F. Wu, "A new bearing fault diagnosis method based on capsule network and Markov transition field/Gramian angular field," Sensors, vol. 21, pp. 7762, November 2021.

[9] N. Barkataki, B. Tiru and U. Sarma, "A CNN model for predicting size of buried objects from GPR B-Scans," J. Appl. Geophys., vol. 200, pp. 104620, May 2022.